ISSN (Online) : 2454 -7190 **ISSN (Print) 0973-8975**
Copyright © J.Mech.Cont.& Math. Sci., Vol.-14, No.-1, January-February (2019) pp 350-364

Ultra Stable and Highly Efficient Nickel Nanotube Catalyst for PEMFC Electrochemical Oxygen Reduction Reaction

[1]Saim Saher, [2]Kamran Alam, [3]Affaq Qamar, [4]Abid Ullah, [5]Waqas A. Imtiaz

[1]Advanced Materials Laboratory (AML), Renewable Energy Engineering (REE), U.S.-Pakistan Center for Advanced Studies in Energy (USPCAS-E), UET Peshawar, Pakistan

[1,2,4]Materials for Energy Storage and Conversion (MESC), U.S.-Pakistan Center for Advanced Studies in Energy (USPCAS-E), UET Peshawar, Pakistan

[3]Electrical Energy System Engineering (EESE), U.S.-Pakistan Center for Advanced Studies in Energy (USPCAS-E), UET Peshawar, Pakistan

[5]Department of Electrical Engineering, Abasyn University, Peshawar, Pakistan

Corresponding author: Dr. Saim Saher
E-mail address: s.saher@uetpeshawar.edu.pk

https://doi.org/10.26782/jmcms.2019.02.00024

Abstract

The oxygen reduction reaction (ORR) in proton exchange membrane fuel cell (PEMFC) having sluggish kinetics at cathode side requires highly active and low cost catalyst. Conventionally, platinum (Pt) is considered to be the most feasible and active catalyst for ORR at cathode, however,it's far expensive to meet the demand for commercialization. Herein novel non platinum group metal (N-PGM) nickel (Ni) nanotubes were prepared by using solvothermal method using transition metal precursor forming Ni ZeoliticImidazolateFramework (Ni/ZIF). Ni nanotubes were obtained after carbonizing Ni/ZIF at 850^{o}C under inert nitrogen atmosphere. The morphology and motif were extensively studied by conducting XRD and SEM. The electro-catalytic performance of Pt/C catalyst, pristine Ni/ZIF and Ni nanotubes were investigated by Linear Sweep Voltammetry (LSV) performed with Rotating Disk Electrode (RDE) in alkaline medium. The Ni/ZIF shows a current density of -1.4 mA/cm^{2}and Ni nanotubes depicts current density of -2.7mA.cm^{-2} and an over potential of -0.27V Vs Saturated Calomel Electrode (SCE). RDE Results were obtained at 400, 800, 1200 and 1600 rpm in 0.1M KOH solution. The evaluation shows that Ni nanotubes own extraordinary electro-catalytic behavior towards ORR activity and Ni nanotubes has potential to be used for PEMFC application.

Key words: Ni ZeoliticImidazolate Framework (Ni/ZIF), Ni nanotubes,Oxygen Reduction Reaction,Linear Sweep Voltammetry

I. Introduction

Due to ever increase in energy consumption; the conventional resources are unable to meet the rising demand of energy around the world. Alternatively, the renewable energy resources coupled with the storage techniques are the way forward to substitute fossil fuels such as coal, natural gas and petroleum. Hydrogen production by solar PV is contemplated for fuel production [I] [II] [III] [VI], which can be readily employed for production of electricity by theproton exchange membrane fuel cell (PEMFC).Interestingly, PEMFC is a promising technology for the conversion of hydrogen to electricity having much higher efficiency than the internal combustion engine and hampering the global pollution in a more effective way.Nonetheless, the use of high cost Pt catalyst and durability hinders its commercialization [X]. Recently, large number of non-platinum materials were studied to enhance the ORR activity and to cope with the harsh environmental condition of fuel cell [IX]. Silver (Ag) was studied due to its abundance, low cost and higher electro chemical activity, however the over potential of Ag in Rotating disk electrode (RDE) is lower than Pt [XIII]. Though the Pt and Ruthenium(Ru) showed higher ORR activity for hydrogen oxidation reaction, converselythey are precious and more prone towards CO poisoning [VIII]. Alloying of transition metals (Co,Fe,Cu,Ni) were also reported to impart synergistic effect to Pt. The d band center of Pt goes down with alloying, decreasing the bonding energy of Pt with oxygenated species [VIII]. K.Yang et al.[XIV] proposed nano-particlesbased PtFe Nitrogen doped carbon sheets (np-PtFe/NPCS), which have three time higher more current density and more positive half wave potential than Pt/C. Y. Haoran et al. [IV] showed a non Pt catalyst for ORR and found its activity better than the commercial Pt/C catalyst. To reduce dependence on the precious metals (Pt, Ru) for ORR, more attention were given to develop non platinum group metals (NPGM) catalysts. H.Jang et al. [VII]illustrated metal organic frame work (MOF) having thermally robust and nano-porous structure, enhancing surface area for reaction. Zeoliticimidazolate frameworks (ZIF's) is a subclass of MOFs which has enormous potential for preparation of nanotube catalyst, which are rich in carbon and nitrogen[I][V].Transition metal carbon nanotubes (Pt-Co CNTs, CoCNT) were developed from ZIF precursors to impart porosity and enhance the catalytic effect of transition metals[XVI] [XVII].X.Zhang et al. [XVIII] investigated Ni catalyst activity alloyed with Co and CNTs ($NiCo_2O_4$/CNTs hybrid), which showed higher performance than Co and CNT [XVIII].

In this study, the novel material ofNickel (Ni) nanotubes synthesized and tested in alkaline solution. Linear sweep voltammetry (LSV) with RDE evaluation were performed to study and analyzed the ORR electro catalytic activities of Ni-nanotubes. The presented results demonstrate Ni nanotubes are the promising catalyst for ORR in PEMFC application.

II. ExperimentalSynthesis of Ni-ZIF

The Ni-ZIF sample prepared by solvothermal synthesis process as described by Xia Bao et al [XV].In this distinctive method a 5.5 g of 2-Methylimidazole (2MIM) is dissolved in 20 ml of deionized (DI) water in a clean beaker. In similar way, 0.238 g of Nickel (II) Nitrate hexahydrate ($Ni(NO_3)_2.6H_2O$) is dissolved in 3 ml of DI water in separate container to obtain a greenish color solution. Later, both the solutions are amalgamated underconstant stirring for 6 h at ambient temperature and pressure. The reaction proceeded with the formation of Ni-ZIF precipitate and soluble salts. The precipitate is separated from the solution by centrifuge action. The soluble nitrates part is flushed by alternatively washing the precipitate by DI water and ethanol till a pH of 7.0 is observed. The precipitate along with some DI water was then transferred to vacuum dryer and kept at a temperature of 80^oC for 24 h to remove the absorbed water from the sample by forced convective mechanism. Ni-ZIF was collected from the container using a spatula and stored in a drying chamber. The flow chart as shown in Fig.1 further elaborates the stepwise synthesis process.

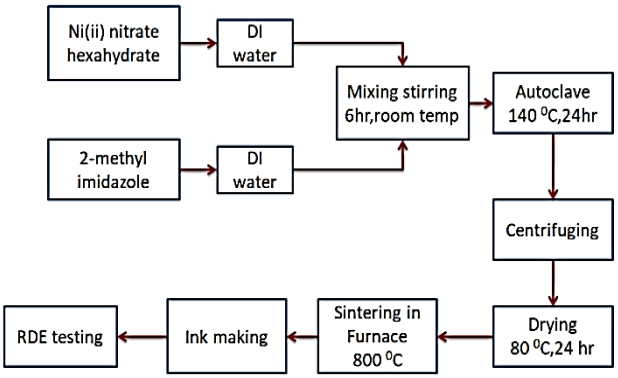

Fig.1 Preparation of Ni-nanotubes

III. Synthesis of Ni nanotubes

As prepared Ni-ZIF sample is placed in a ceramic boat inside a controlled environment tube furnace. The sealed furnace is flushed with nitrogen gas for 3 h at room temperature to desorb the gases from Ni-ZIF sample in order to avoid oxidation. The furnace is set at 350^oC with a ramp rate of 5$^oC.min^{-1}$ for 1.5 hours dwell time in nitrogen atmosphere. The furnace temperature is then raised to 800^oC a ramp rate of 5$^oC.min^{-1}$ and dwelled for 4 h under steady supply of nitrogen gas. During this process structural transformation occurs in the ZIF ligand. Later, the furnace is cooled to ambient temperature in free convection manner and the Ni-nanotubes are collected in a contaminant free container.

IV. Leaching of Ni nanotubes

The calcinated Ni-nanotubes immersed in a 0.5 M solution of sulphuric acid to remove unreacted part of the metal from the sample. The solution is forced through

filtered in vacuum assisted system and subsequently washed with DI water to ensure no traces of acid are present in the specimen. The Ni-nanotube powder is dried in the vacuum oven for 12 h at 80^{o}C [XI].

V. Ink Preparation

Catalytic ink is prepared by interspersing a 7.6 mg of Ni nanotubes sample in 7.6 ml of DI water. A 2.4 ml isopropanol alcohol (IPA) along with 40 μL of 5 wt% of Nafion (LQ-1005-1000, Ion power Inc.) mixed in the solution to enhance the ionic conductivity and to assist the layer adhesion of catalyst ink with glassy carbon. The solution was sonicated for 30 min in cold water prior to applying on the glassy carbon surface [XII].

VI. Experimental setup

Linear sweep voltammetry tests were conducted on rotating disk electrode (RDE) immersed in 0.1 M KOH inside a three compartment glass vessel. Standard calomel electrode (SCE) is opted as reference electrode, platinum (Pt) wire was used as counter electrode, while catalyst layer deposited on the GC (4mm diameter) is used as working electrode.

VII. Working Electrode preparation

A small amount of the catalyst ink is applied onto the surface of the glassy carbon disk having 4 mm diameter (AFE3T040GC, Pine Instruments). The catalyst layers are dried using heater and fan [XII], resulting in a catalyst loading of 0.7mgand tests were conducted at room temperature and pressure. Prior to each test the oxygen was purged through the electrolyte for 30 min in a steady state flow during the experiments. Linear Sweep Voltammograms (LSV) was generated at the potential sweep of -0.3 to 0.7 V at 20 $mV.s^{-1}$ scan rate at different rpm. LSV obtained for different catalyst loading to realize an optimized value of loading for higher ORR activity, higher current density and to find a balance in mass transport density and conductivity of the catalyst layer. This research is aimed at achieving volumetric activity of greater or equal to 1 by 10th of the Pt based catalyst. Tests were performed for 500 cycles for the same layer of sample on Glassy carbon (GC) to find out the durability of the catalyst in alkaline medium.

VIII. Characterization

The morphology and crystalline structure of Ni nanotubes were investigated under Field Emission Scanning Electron Microscopy (FEI Quanta 250 FEG Scan).The powder X-ray diffraction (XRD) were conducting using D8 Bruker X-Ray Diffractometer (PW1830 Netherland) with CuK$\boldsymbol{\alpha}$ radiation (Cu kα, ƛ=0.154nm, 40 kV and 30mA) and linear sweep voltammetry was performed by using RDE setup (AFE 3T040GC, Pine instruments with 4mm diameter GC).

IX. Results and Discussion

The microstructure of the solvothermally prepared Ni nanotubes is investigated by scanning electron microscopy (SEM) as shown in Fig. 2. The dichotomous bamboo shaped nanotubes having approximate width and length of 10-12µm and 100 nm respectively. The morphology shows that Ni nanotubes are formed through the thermal transformation of Ni/ZIF sample. The nanotubes having large length and small diameter results in higher aspect ratio, henceforth increases the surface area and enhances the electro catalytic activity.

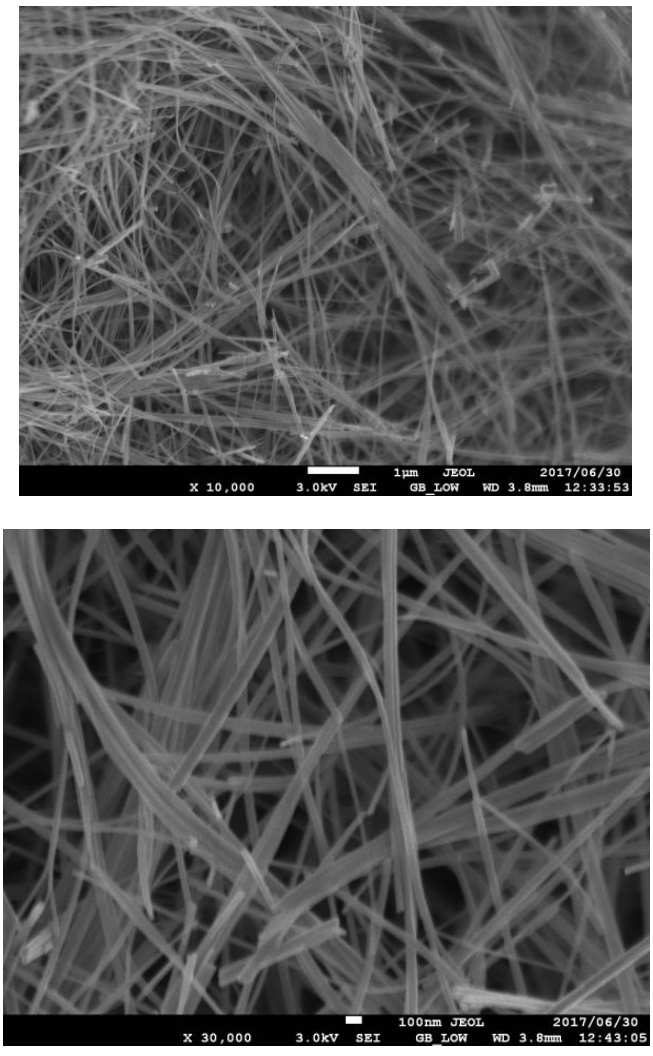

Fig. 2 Scanning electron micrographs of Ni nanotubes

Fig. 3 represents the powder X-Ray Diffraction (XRD) pattern of Ni nanotubes catalyst. The sharp diffraction peak at 45.5^{o}corresponds to (200) graphite plane. The distinct peaks at 38.3^{o},52.6^{o},76.8^{o} matches with (111), (220), (222) indicating the presence of crystalline carbon and metallic Nickel.No metallic carbide, oxide peak were observed showing absences of these elements.

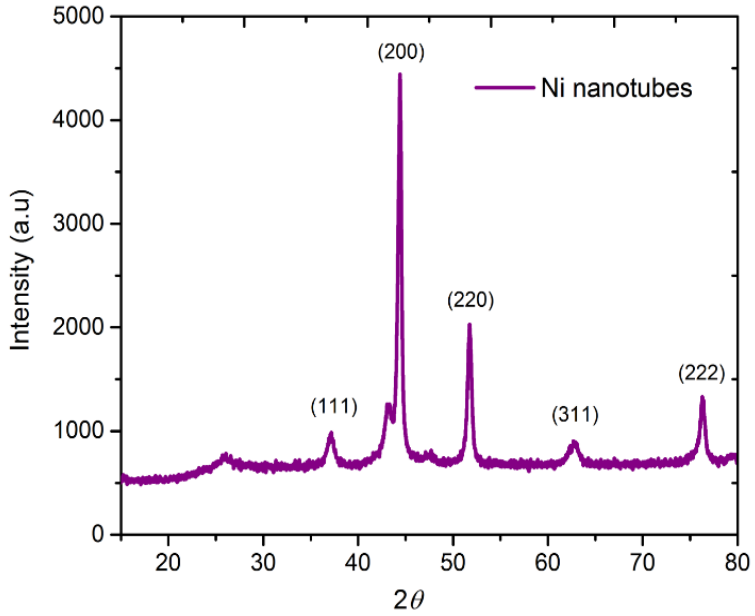

Fig.3 X-Ray Diffraction (XRD) pattern of Ni nanotubes

X. ORR Performance

The ORR activity and stability of nickel nanotubes were evaluated through linear sweep voltammetry in nitrogen saturated 0.1M KOH electrolyte in conventional tri electrode system by AFE32040GC, Pine Instruments. A glassy carbon (GC) electrode was used as working electrode. The Pt foil and saturated calomel electrode were used as counter and reference electrode respectively. To prepare working electrode, 7.6mg of catalysts were dispersed in a mixture of 7.6ml of DI water, 2.4 ml isopropanol alcohol and 40µl of nafion solution is ultrasonicated for 30 min. Afterward,10 µl of obtained catalyst ink was deposited on GC substrate. For the LSV tests, oxygen was pre-adsorbed on the GC electrode coated with electro-catalyst by bubbling in the electrolytes for 30 min. The kinetic mechanism and durability of nickel (Ni) nanotubes towards ORR is evaluated by linear sweep voltammetry (LSV) in a tri electrode system. For comparison purpose the LSVof Ni/ZIF and Pt/C commercial catalyst were also conducted in similar environment. The Fig. 4, 5 and 6 shows the ORR activity of Ni nanotubes, Ni/ZIF and commercial Pt/C catalysts,respectively, in O_2 saturated electrolyteat different rpm.

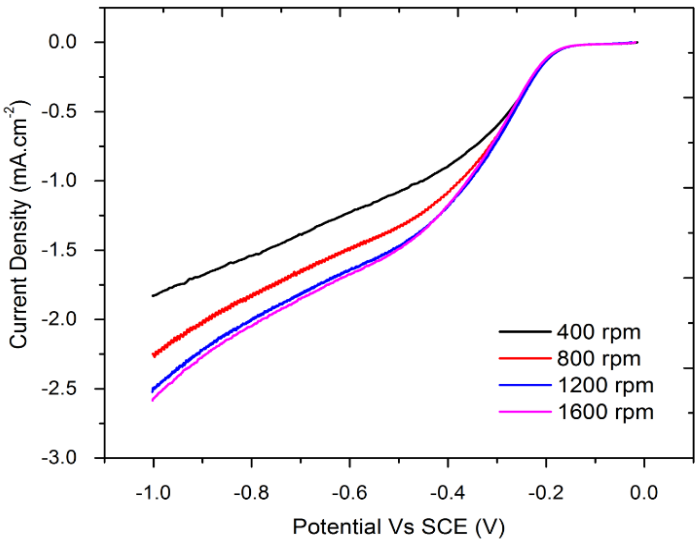

Fig.4RDE data of Ni nanotubes

The ORR activity of Ni nanotubes is shown in Fig. 4 at 400, 800, 1200, 1600 rpm in oxygen saturated electrolyte. The current density reaches -2.7mA.cm^{-2} at 1600 revolution (rpm). The current density slowly increases from 400 rpm to maximum at 1600 rpm.

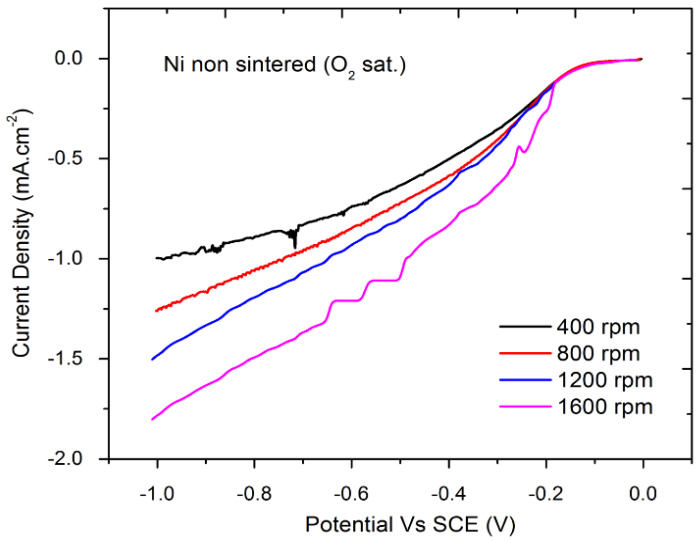

Fig.5RDE data of Ni/ZIF non sintered

While the current density of Ni/ZIF in the same environment reaches to -1.7 mA.cm^{-2} at 1600 rpm (see Fig. 5).The current density of Ni nanotubes increaseswith the heat treatment of Ni catalyst. The enhancement in current density is because of the transformation of Ni/ZIF to Ni nanotubes and increase in surface area.

Fig. 6 demonstratesthe Pt/C catalyst has the highest current density of -4.6mA.cm^{-2} inthe same environment, which is quite high due to the abundance andinexpensiveness of Ni nanotubes. Although, the current density of Ni nanotubes is lower with respect to Pt/C, however, by increasing the loading content of Ni nanotubes this deficiency can be overcome.

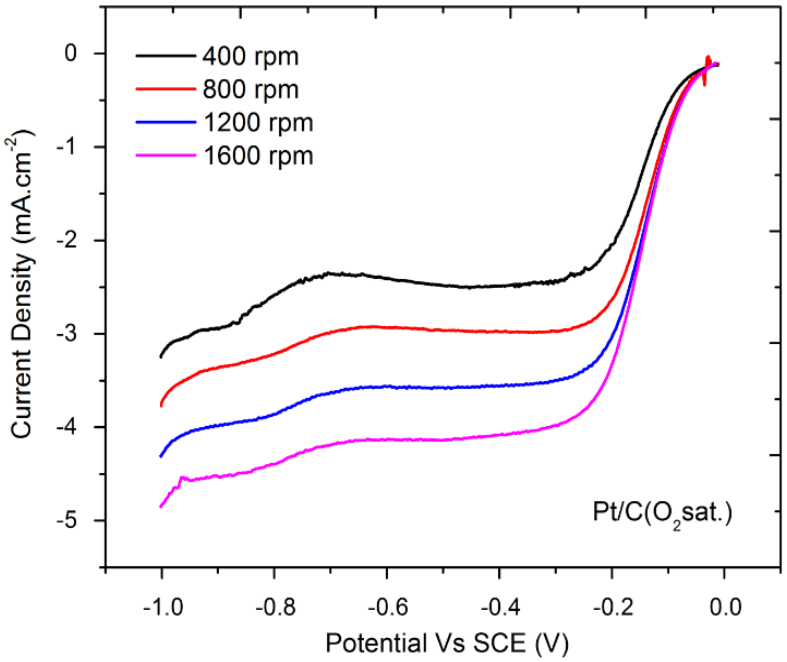

Fig.6RDE data of Pt/C all at various rpm

The comparison purpose all the three catalysts are sum-up inFig. 7, which indicates the highest current density of Pt/C.Interestingly, Ni nanotubes have shown greater current density than Ni/ZIF,clearly indicating the treatment effect on the Ni catalyst.

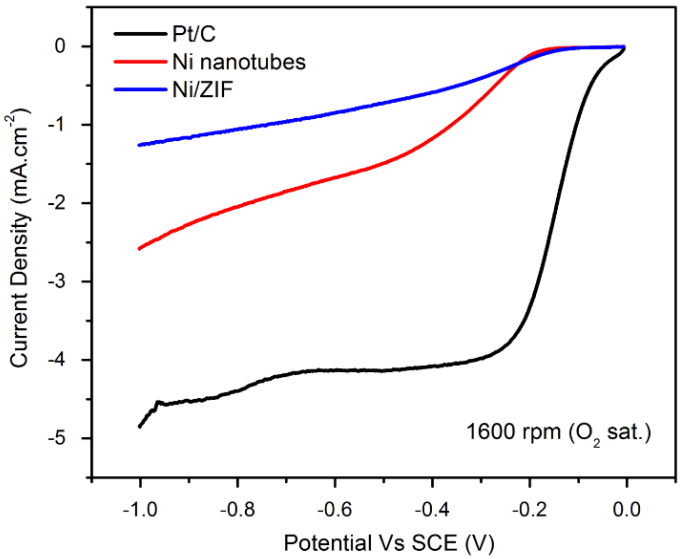

Fig.7Comparison of Ni nanotubes, Ni ZIF and Pt/C at 1600 rpm

In order to evaluate the electron number the Koutecky-Levich(K-L) plot is drawn between the inverse of current density and rotation data acquired from RDE of Ni nanotubes in oxygen concentrated electrolyte, as shown in Fig. 8.The extrapolation of the K-L plot gives us an intercepts adjacent to zero (0), which demonstrate that the process of oxygen (O_2) reduction is totally under the diffusion control, and the slop B.

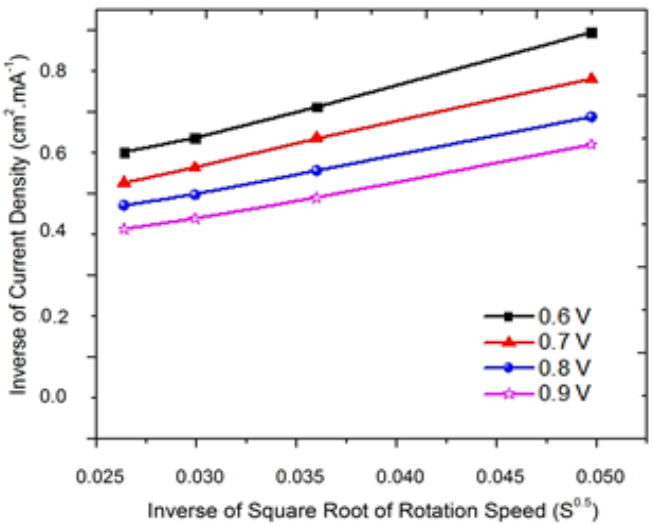

Fig.8K-L plot for Ni nanotubes at various potentials

Fig. 9 shows the K-L plot for the Ni ZIF. This indicated that the intercept is above zero, so the oxygen reduction is not only under the control of diffusion.

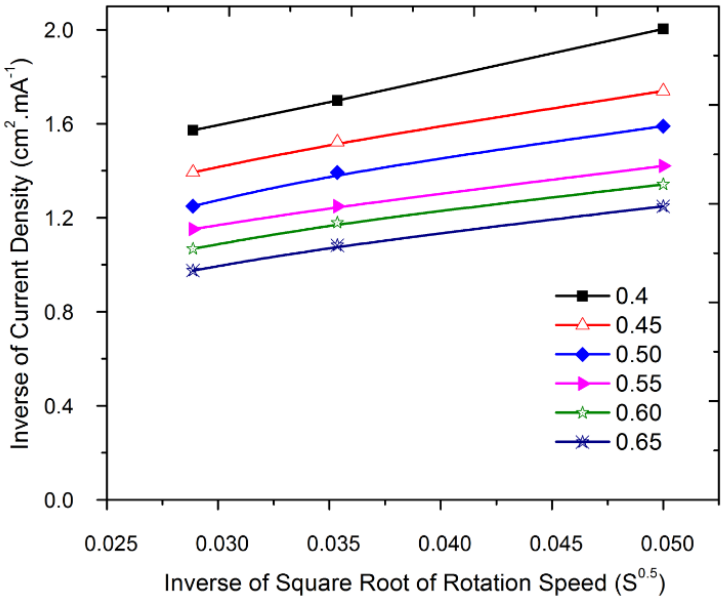

Fig. 9K-L plot for Ni ZIF at various potential

The electron transfer number is then calculated by plugging the values in the equation 1 to 4. The charge transfer number come up between 3 and 4 for Ni nanotubes, which indicates the oxygen is converting directly to water without forming peroxide. Fig. 8 shows that the value for oxygen reduction potential for Ni nanotubes approaches to 4 at higher potential, showing direct ORR to water without any peroxide generation at the higher potential range. While the electron number is between 2 to 3 for Ni/ZIF indicating the oxygen reduction proceeds in two pathways, it produces peroxide parallel with water making the internal environment caustic. ORR will either occur via the 4 electron reduction pathway where O_2 is reduced to water or the 2-electron reduction pathway where it is reduced to hydrogen peroxide (H_2O_2).In PEMFC the 4-electron direct pathway is more desirable. Herein, 4 electron transfer can be achieved at higher potential range.

$$1/J = 1/J_L + 1/J_K \quad (1)$$

$$= 1/B\ \omega^{-1/2} + 1/J_K \quad (2)$$

$$B = 0.62\ N\ F\ C_0\ (D0)^{2/3}\ \upsilon^{-1/6} \quad (3)$$

$$J_K = n\ F\ k\ C_0 \quad (4)$$

J is the overall current density, J_K and J_L are the kinetic and diffusion- Limiting current densities, ω is the angular velocity of the disk (ω =2πN, N is the linear rotation speed), n is the overall charge transferred number in oxygen reduction, F is the Faraday constant (F = 96485 C.mol^{-1}), C_0 is the bulk concentration of O_2 , υ is the kinematic viscosity of electrolyte, and k is the electron transfer rate constant. As from the Fig. 7 the charge transfer number(n) and J_K can be calculated from the slop and intercept of the K-L plots respectively, and by using parameters C_0 =1.2 × 10^{-3}mol L^{-1}, D_0 = 1.9 × 10^{-5} cm s^{-1} and υ = 0.1 m^2 s^{-1} in 0.1 M KOH.

To know about the kinetics of electron transfer of Ni nanotubes and Ni ZIF during the ORR, we have studied the reaction kinetics by rotating disk voltammetry. The voltammetry profile in O_2 saturated 0.1 M KOH electrolyte shows that the current density is enhanced by an increase in rotation rate from 400 to 1600, as shown in Fig. 4.

The corresponding K-L plots (J^{-1}Vs $\omega^{-1/2}$) at different electrode potentials (see Fig. 7) depicts good linearity and parallelism of the plots are considered as example of first order reaction kinetics in regard to the concentration of mixed O_2. The kinetic parameters can be examined on the basis of Koutecky-Levich equations.

The durability can be examined by comparing the LSV of Ni nanotubes for first cycle and 1000th cycle as represented in Fig. 10. It is shown the degradation is only 2% which is very smaller than degradation ofPt/C [XI]

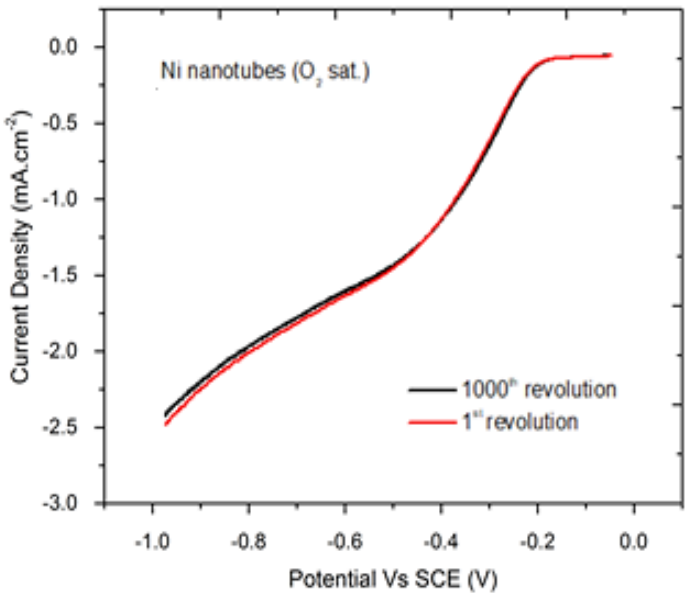

Fig.10 LSV data for Ni nanotubes showing degradation after 1000th cycle

From Fig. 11, full width half maximum (FWHM) was calculated. From the data the crystal size was then calculated through Scherrer equation

$$D = K\lambda / (d \cos\theta) \qquad \text{Scherrerequ.}$$

D is the crystal size, K is shape factor close to unity (0.9), λ is the X-ray wave length (λ = 1.54060 for Cu kα), d is broadening at half maximum intensity (units are in radians), θ is Bragg angle. By using the above equation the crystal size calculated is 3-4nm. They have broader peaks and smaller crystallite size resulting in an enhanced activity.

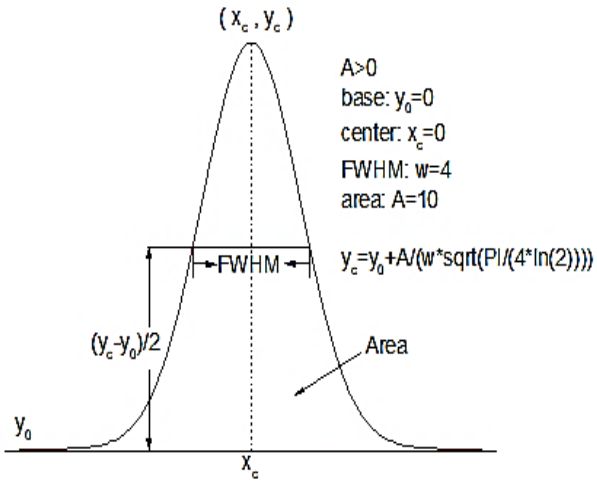

Fig. 11 Full width half maximum (FWHM)

Diffusion time is effected by the crystallite size, according to average diffusion time equation larger particle size require larger diffusion time and vice versa shown by the equation below

$$T = r^2 \pi^2 D \qquad \text{average diffusion time equation}$$

Herein the crystallite size is small leads to smaller diffusion time, thus enhancing catalytic activity.

XI. Conclusions

Ni nanotubes were prepared by hydrothermal treatment and sintering at 850 ^{o}C in N_2 environment. As illustrated from RDE analysis, the Ni nanotubes catalyst depicts extra ordinary catalytic behavior towards ORR as compared to the Ni ZIF. Although, the presented activity is lower than Pt/C catalyst,nonetheless, thisshortfall can be resolved by the increase of loading content. As shown from LSV, the

degradation ismuch lower even after several hundred cycles and the catalyst is stable in comparison to Ni ZIF and Pt/C under identical conditions. The catalyst shows higher ORR and seemed to be potentialcontender for oxygen reduction at cathode side of PEMFC.

XII. Acknowledgement

The authors wish to thank the researchers whose literature has been cited in this article and acknowledge Materials for Energy and Sustainability Research Group for providing materials and experimental setups used in this study. Research leading to this article was supported by the research grants of U.S.-Pakistan Center for Advanced Studies in Energy (USPCASE), UET Peshawar and U.S. Agency for International Development, USAID (AID-391-A-14-000007) under the project title "Synthesis of nanofluid to improve the thermal and D.B.S. of T.O".

Refernces

I. Cheng, F., & Chen, J. (2012). Metal–air batteries: from oxygen reduction electrochemistry to cathode catalysts. *Chemical Society Reviews*, *41*(6), 2172-2192.

II. Fekete, M., Hocking, R. K., Chang, S. L., Italiano, C., Patti, A. F., Arena, F., &Spiccia, L. (2013). Highly active screen-printed electrocatalysts for water oxidation based on β-manganese oxide. *Energy & Environmental Science*, *6*(7), 2222-2232.

III. Gorlin, Y., & Jaramillo, T. F. (2010). A bifunctional nonprecious metal catalyst for oxygen reduction and water oxidation. *Journal of the American Chemical Society*, *132*(39), 13612-13614.

IV. Haoran, Y., Lifang, D., Tao, L., & Yong, C. (2014). Hydrothermal synthesis of nanostructured manganese oxide as cathodic catalyst in a microbial fuel cell fed with leachate. *The Scientific World Journal*, *2014*.

V. He, G., Qiao, M., Li, W., Lu, Y., Zhao, T., Zou, R., &Parkin, I. P. (2017). S, N- Co- Doped Graphene- Nickel Cobalt Sulfide Aerogel: Improved Energy Storage and Electrocatalytic Performance. *Advanced Science*, *4*(1), 1600214.

VI. Iyer, A., Del-Pilar, J., King'ondu, C. K., Kissel, E., Garces, H. F., Huang, H., &Suib, S. L. (2012). Water oxidation catalysis using amorphous manganese oxides, octahedral molecular sieves (OMS-2), and octahedral layered (OL-1) manganese oxide structures. *The Journal of Physical Chemistry C*, *116*(10), 6474-6483.

VII. Kjaergaard, C. H., Rossmeisl, J., &Nørskov, J. K. (2010). Enzymatic versus inorganic oxygen reduction catalysts: Comparison of the energy levels in a free-energy scheme. *Inorganic chemistry*, *49*(8), 3567-3572.

VIII. Kundu, S., Nagaiah, T. C., Xia, W., Wang, Y., Dommele, S. V., Bitter, J. H., &Muhler, M. (2009). Electrocatalytic activity and stability of nitrogen-containing carbon nanotubes in the oxygen reduction reaction. *The Journal of Physical Chemistry C*, *113*(32), 14302-14310.

IX. Liao, L., Zhang, Q., Su, Z., Zhao, Z., Wang, Y., Li, Y., &Cai, X. (2014). Efficient solar water-splitting using a nanocrystallineCoOphotocatalyst. *Nature nanotechnology*, *9*(1), 69.

X. Mukerjee, S., &Srinivasan, S. (1993). Enhanced electrocatalysis of oxygen reduction on platinum alloys in proton exchange membrane fuel cells. *Journal of Electroanalytical Chemistry*, *357*(1-2), 201-224.

XI. Shi, X., Iqbal, N., Kunwar, S. S., Wahab, G., Kasat, H. A., &Kannan, A. M. (2018). PtCo@ NCNTs cathode catalyst using ZIF-67 for proton exchange membrane fuel cell. *International Journal of Hydrogen Energy*, *43*(6), 3520-3526.

XII. Shinozaki, K., Zack, J. W., Richards, R. M., Pivovar, B. S., &Kocha, S. S. (2015). Oxygen reduction reaction measurements on platinum electrocatalysts utilizing rotating disk electrode technique I. Impact of impurities, measurement protocols and applied corrections. *Journal of The Electrochemical Society*, *162*(10), F1144-F115

XIII. Su, B., Hatay, I., Trojánek, A., Samec, Z., Khoury, T., Gros, C. P.,&Girault, H. H. (2010). Molecular electrocatalysis for oxygen reduction by cobalt porphyrins adsorbed at liquid/liquid interfaces. *Journal of the American Chemical Society*, *132*(8), 2655-2662.

XIV. Song, E., Shi, C., & Anson, F. C. (1998). Comparison of the behavior of several cobalt porphyrins as electrocatalysts for the reduction of O2 at graphite electrodes. *Langmuir*, *14*(15), 4315-4321.

XV. Xia, B. Y., Yan, Y., Li, N., Wu, H. B., Lou, X. W. D., & Wang, X. (2016). A metal–organic framework-derived bifunctional oxygen electrocatalyst. *Nature Energy*, *1*(1), 15006.

XVI. Yang, J., Sun, H., Liang, H., Ji, H., Song, L., Gao, C., &Xu, H. (2016). A highly efficient metal- free oxygen reduction electrocatalyst assembled from carbon nanotubes and graphene. *Advanced Materials*, *28*(23), 4606-4613.

XVII. Zhang, W., Shaikh, A. U., Tsui, E. Y., &Swager, T. M. (2009). Cobalt porphyrin functionalized carbon nanotubes for oxygen reduction. *Chemistry of Materials*, *21*(14), 3234-3241.

XVIII. Zhang, X., Chen, Y., Wang, J., &Zhong, Q. (2016). Nitrogen and fluorine dual- doped carbon black as an efficient cathode catalyst for oxygen reduction reaction in neutral medium. *ChemistrySelect*, *1*(4), 696-702.